A Unified Approach to Quantification by Kinetic Analysis in Nuclear Medicine

A. M. Peters

Department of Diagnostic Radiology, Hammersmith Hospital, London, England

J Nucl Med 1993; 34:706–713

The greatest attribute of nuclear medicine is its ability to quantify physiological processes noninvasively. As Dr. Keith Britton said at the 1986 annual meeting of the European Association of Nuclear Medicine, "Nuclear medicine has time." Time is probably the single most important variable in nuclear medicine with the other two being volume and mass. These three variables are related to each other by three equations of fundamental importance:

$$T = V/Q, \quad \text{Eq. 1}$$

$$C = M/V, \quad \text{Eq. 2}$$

and

$$\frac{dM}{dt} = Q(C_a - C_v), \quad \text{Eq. 3}$$

where T is mean transit time, V is volume of distribution, Q is blood flow, C is concentration, M is mass (mg or MBq) and the subscripts a and v refer to arterial and venous, respectively.

The third equation is an example of the Fick principle: when an indicator is introduced into a system, it must be subject to the conservation of matter within the system or, in the usual nuclear medicine setting, the rate of change of organ content of a tracer is equal to the difference between the organ input rate and output rate of the tracer.

It is remarkable, as this review is intended to show, how a substantial proportion of quantitative nuclear medicine stems from these three equations.

TIME

Mean transit (or residence) time is the basis of many measurements made in nuclear medicine. Some variables are expressed as such or are combinations of time with volume or mass giving flow rates and flux rates.

There are two approaches to the measurement of mean transit time: outflow detection and residue detection. With residue detection, the fraction remaining of a tracer instantaneously deposited in an organ is monitored externally. Mean tracer transit time (T) through or residence time within the organ is then the ratio of the total area under the residue curve and its initial height, i.e., the y value at zero time (*1*). Because the units of an area are those of the product of x and y axes, the area-to-height ratio must have x-axis units (i.e., time), whatever the units of the y-axis, since the latter cancel out.

Measurement of transit time by residue detection requires that the tracer be deposited instantaneously in the organ or tissue so that the entire dose can be represented by the initial count rate (height) of the residue curve (Fig. 1). It also requires that the residue curve be uninterrupted by recirculation of the tracer. There are many examples in nuclear medicine of mean transit time measurement by residue detection, including tissue perfusion measurement by inert gas washout after local arterial injection and pulmonary alveolar permeability following inhalation of radiolabeled aerosol. The requirements of instantaneous injection and no recirculation are met in these two examples. In other situations where a recirculating tracer is given intravenously, it is necessary to indirectly estimate the curve that would have been obtained had the tracer been injected directly into an artery supplying the organ and did not recirculate. By using deconvolution analysis, this can be done by recording the time-activity curve over the organ and in the blood (usually from a region of interest (ROI) over the left ventricle (*2*). If the tracer disappears from the organ monoexponentially, T is also equal to the reciprocal of the rate constant of disappearance (Fig. 1).

Measurement of transit time by outflow detection involves the construction of a time-concentration curve from the effluent of an organ following instantaneous injection of tracer upstream in an afferent artery. Such a curve can be converted to a residue curve by integrating it backwards, i.e., from infinite time back to zero time (Fig. 2). Again, T is the area under the integrated curve

Received Apr. 21, 1992; revision accepted Oct. 22, 1992.
For reprints or correspondence contact: A. M. Peters, Dept. of Diagnostic Radiology, Hammersmith Hospital, DuCane Rd., London W12 0HS, England.

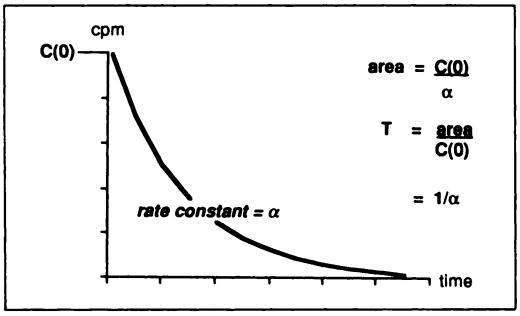

FIGURE 1. A time-activity (residue) curve recorded following instantaneous injection of a tracer into an organ (possibly blood). Because it is deposited instantaneously, the dose is proportional to the initial count rate (initial height of the curve), shown here as C(0). The longer the tracer takes to leave the organ, the greater the total area under the residue curve will be. The mean residence time, T, of the tracer in the organ is equal to the area under the curve divided by its initial height. This is intuitively evident since an area has units which are the product of the x- and y-axis units and when it is divided by the y-axis variable, the y-axis units cancel out. Furthermore, since the area under a monoexponentially decreasing curve is equal to its initial height divided by its rate constant, the latter is equal to the reciprocal of the mean transit time for such a curve.

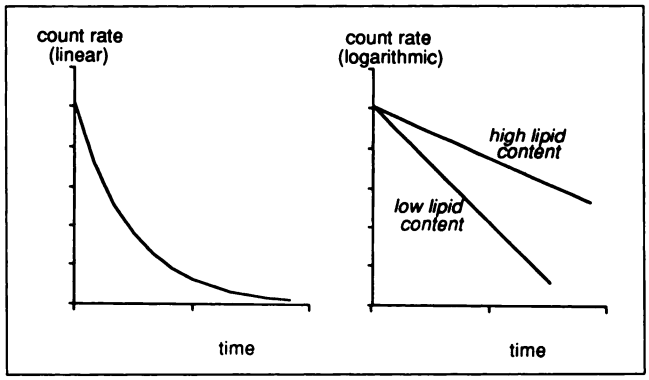

FIGURE 3. (Left) Idealized monoexponential residue curve recorded after injection of inert gas into an organ and expressed on a linear y-axis. (Right) Two idealized monoexponential residue curves expressed on a logarithmic y-axis after injection of inert gas into two organs with identical perfusion but with differing lipid contents. The high lipid-content organ tends to retain gas because of the latter's higher lipid solubility. This gives the organ a higher effective gas distribution volume. So, whereas the lower lipid-containing organ 1/T is equal to Q/V, it is equal to Q/σV for the higher lipid-containing organ, where σ is the ratio of the solubilities of the gas in the tissue and blood (taken to be unity for the organ with less lipid).

divided by its initial height. Transit time measured by this approach is almost always combined with simultaneous measurement of either volume (by dilution) to generate flow (as in the measurement of cardiac output) or flow to generate volume (as in the measurement of lung water with labeled water, flow being cardiac output) (*3*).

In contrast to outflow detection, T measured by residue detection is frequently expressed as such (for example, in tissue perfusion measurements using ^{133}Xe). Since perfusion is Q/V (ml/min/ml) from which volume cancels out, it is the reciprocal of transit time and is actually measured as the mean residence time of ^{133}Xe in the organ. If the solubility of the ^{133}Xe in the tissue is high and exceeds that in blood (Fig. 3), then T will tend to be prolonged. Therefore, T is actually equal to Q/σV where σ is the partition coefficient of ^{133}Xe between tissue and blood. Assuming equilibration of ^{133}Xe between tissue and capillary blood, $C_v = C_t/\sigma$, where C_t is tissue concentration. Sometimes σV is called the effective volume of distribution of the gas.

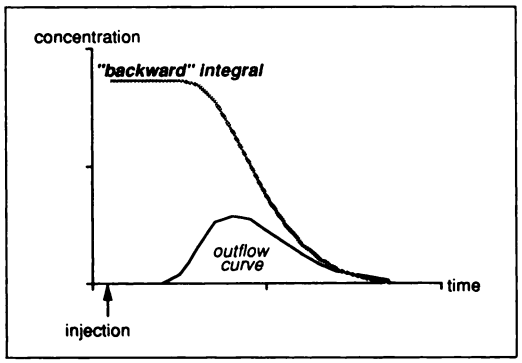

FIGURE 2. Mean transit time of a tracer through an organ can be obtained from the time-concentration curve recorded by continuous measurement of the concentration of tracer in the blood draining the organ. Integration backwards of such an outflow curve (i.e., towards zero time instead of towards infinity) reproduces the residue curve that would have been obtained if the tracer had been monitored by external detection while it was contained within the organ. The duration of the initial plateau is the *minimum* transit time through the organ.

The relationship between Q/V and T can also be derived from the Fick principle. Thus, if M_t is the amount of ^{133}Xe remaining in the tissue after injection, then

$$dM_t/dt = Q(C_a - C_v). \qquad \text{Eq. 4}$$

Since recirculation is prevented by retention of gas in the lung, C_a is zero, and so

$$dM_t/dt = -Q.C_v. \qquad \text{Eq. 5}$$

Since $C_v = C_t/\sigma$, we can say

$$dM_t/dt = -Q.C_t/\sigma, \qquad \text{Eq. 6}$$

and since

$$C_t.V = M_t, \qquad \text{Eq. 7}$$

then

$$\frac{dM_t}{dt} = -\frac{Q.}{\sigma V} M_t, \qquad \text{Eq. 8}$$

where V is the distribution volume of tracer within the tissue (which for the highly diffusible ^{133}Xe is the tissue volume itself). Note the minus sign in Equations 5, 6 and 8 which indicates that the activity in the tissue is *decreasing*.

When the rate of change of a variable is proportional to that variable, as in Equation 8, the rate of change is exponential with, in the above case, a rate constant of $Q/\sigma V$. This rate constant is also 1/T.

The mean residence time of ^{133}Xe in a heterogeneously perfused tissue, such as the kidney [provided that ^{133}Xe is deposited instantaneously in all (parallel) compartments (*4*)], is still equal to total area divided by total initial height even though the resulting washout curve is multiexponential.

The measurement of $Q/\sigma V$ under steady-state conditions, during a continuous infusion of a short-lived tracer such as $H_2{}^{15}O$, is also a residence time measurement in which the residence time of the tracer in the organ is compared with the physical lifespan of the tracer. Again, the relationship between perfusion and the tissue tracer concentration which becomes constant under steady-state conditions can be derived from the Fick principle.

Thus, $$dM_t/dt = Q(C_a - C_v) - C_t.V.\lambda, \qquad \text{Eq. 9}$$

where λ is the physical decay constant of the radionuclide.

At equilibrium, $\frac{dM_t}{dt} = 0.$

If the tracer equilibrates between venous blood and tissue, then

$$Q.C_a - Q.C_t/\sigma - C_t.V.\lambda = 0. \qquad \text{Eq. 10}$$

Rearranging

$$\frac{C_t}{C_a} = \frac{Q/V}{(Q/\sigma V) + \lambda}. \qquad \text{Eq. 11}$$

For tissues in which $Q/\sigma V$ is small compared with λ, C_t is proportional to Q/V and the image portrays blood flow distribution. With respect to the lung, Q can be replaced by ventilation, $\dot{V}$, and plasma concentrations by gas concentrations. It can then be seen that, for a short-lived gas like ^{81m}Kr, the lung image portrays the distribution of ventilation (*5*) in relation to lung volume, V,

i.e. $$\frac{C_{alv}}{C_{insp}} = \frac{\dot{V}/V}{\dot{V}/V + \lambda}. \qquad \text{Eq. 12}$$

Blood clearance studies are special cases of mean transit time measurement by residue detection in which the tracer is instantaneously deposited into the intravascular compartment. For tracers with a distribution volume confined to the intravascular space, T is equal to V/Z, where V is now plasma volume and Z is the blood clearance. In other words, clearance is a variable with units of flow and represents in this context the volume of circulating blood cleared of the tracer per unit of time, i.e., it is a virtual blood flow. With respect to Equation 1, Q and Z are equivalent and interchangeable variables.

Several variants of clearance are encountered in the literature including whole body clearance, organ clearance, urinary clearance and blood clearance. Organ clearance of a tracer is equivalent to the blood flow of the organ that would be required to accumulate the tracer at the observed rate if the extraction fraction, E, of the tracer was unity. Therefore, Z = Q.E and Z = Q if E is unity. If several organs remove tracer from blood, then we can say that the sum of their Q.E products is the whole body clearance and is identical to blood clearance. Urinary clearance is the virtual flow rate of blood to the kidney completely extracted of tracer which ultimately appears in the urine. It cannot exceed renal clearance. The term plasma clearance is reserved for tracers that do not enter red cells and is related to blood clearance simply by the hematocrit. The mean residence time of a tracer in blood is equal to the blood volume divided by the blood clearance and, provided the tracer is deposited instantaneously into the intravascular compartment, is equal to the area under the blood concentration-time curve divided by the zero time concentration. Alternatively, mean transit time in blood can be derived from the Fick principle as the reciprocal of the rate constant of blood disappearance if this is monoexponential (see Equation 20).

As stated above, T is only equal to V/Q or V/Z if mixing is instantaneous. An example of a situation where mixing of a tracer throughout its final distribution volume is not instantaneous is DTPA (or EDTA) throughout the extracellular fluid volume (ECF). These filtration markers take 1–2 hr to mix throughout the ECF. This gives rise to a bi-exponential plasma disappearance curve (Fig. 4). The total area under the plasma disappearance curve divided by the initial height is *not* equal to mean residence

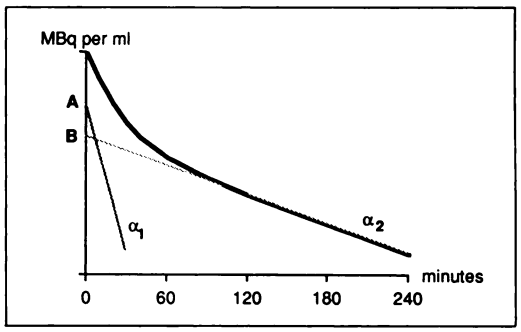

FIGURE 4. A bi-exponential disappearance curve, such as would be recorded in plasma following injection of ^{99m}Tc-DTPA or ^{51}Cr EDTA for the measurement of glomerular filtration rate (GFR). The area under a bi-exponential curve is equal to the sum of the areas under each exponential:

$$\frac{A}{\alpha_1} + \frac{B}{\alpha_2}$$

then

$$GFR = \frac{\text{mass injected}}{A/\alpha_1 + B/\alpha_2}.$$

time in the ECF but to the mean residence time in *plasma* (in which mixing of the tracer *is* instantaneous), i.e., to plasma volume divided by GFR.

Thus, in any system, several specific definitions of mean transit time may be possible. With regard to plasma clearance studies, it is necessary to make a distinction between sojourn time and residence time. A prime example would be a molecule of DTPA passing to and fro between plasma and interstitial fluid. Sojourn time is the average time it spends in either compartment before returning to the other. Residence time in either compartment is the *total* time spent in that compartment before undergoing glomerular filtration. The *sum* of the residence times in plasma and interstitial fluid is the residence time in the ECF. Sojourn time and residence time are identical in systems where the tracer is confined to plasma and disappears unidirectionally, such as colloid taken up in the liver. In the case of DTPA, sojourn time is important since its measurement reflects the average permeability surface area product (of the whole body) for the molecule. Thus, taking the general equation, T = V/Q, sojourn time in plasma is plasma volume divided by the sum of the clearances into the extravascular extracellular space and into the kidney (i.e., GFR). The mean residence time of DTPA in the ECF is ECF volume divided by GFR. It is obtainable from the plasma disappearance curve, C(t), as the moment, $\int$ t. C(t).dt/ $\int$ C(t).dt, from which it can be shown (*6*) that

$$T_{ECF} = \frac{A/\alpha_1^2 + B/\alpha_2^2}{A/\alpha_1 + B/\alpha_2}, \qquad \text{Eq. 13}$$

where A and B are the zero time intercepts and α_1 and α_2 are the rate constants of the bi-exponential plasma disappearance curve (Fig. 4). Because it is equal to Q/V, the reciprocal of T as applied to the mean residence time of DTPA in the ECF is an alternative form in which to express GFR; i.e., normalized to ECF volume instead of body surface area. Because α_2, the rate constant of the second exponential of the plasma DTPA (or EDTA) clearance curve is very nearly equal to $1/T_{ECF}$, it represents a simple, convenient, accurate and physiological means of measuring GFR (*7*).

VOLUME

Measurement of volume is usually by means of tracer dilution, i.e., using Equation 2. Examples include blood volume, total body water and the exchangeable sodium space. It is also occasionally measured from separate measurements of T and Q using Equation 1 for the measurement of lung water (where Q is cardiac output) and extracellular fluid volume (where Q is GFR). Volume is also measured directly from PET and SPECT by summation of slice areas, although this is a fundamentally different approach compared with the kinetic approach which is the theme of this article.

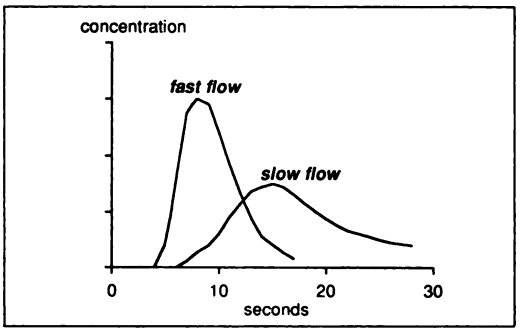

FIGURE 5. Principle of blood flow measurement by the indicator dilution technique. The area under the outflow concentration-time curve is directly proportional to the transit time of the blood (i.e., to the reciprocal of its velocity) and inversely proportional to the volume of blood within which the tracer is diluted. It appears as the denominator in the indicator dilution equation:

$$\text{flow} = \frac{\text{mass injected}}{\text{area}}.$$

The two idealized curves represent dilution curves for the same blood flow (equal masses injected) for a large volume of blood moving slowly and a small volume of blood moving rapidly.

Volume is frequently measured as one component of blood flow measurement by the dilution principle. Techniques for measuring *absolute* blood flow in which volume must be measured (in contrast to *perfusion*, or as a *fraction* of cardiac output) include the Fick principle, indicator dilution (Stewart-Hamilton), blood clearance and isotope plethysmography. The indicator dilution technique uses outflow detection to derive the time component of flow and measures the volume by dilution (Fig. 5). It can be illustrated by the Stewart-Hamilton technique for measuring cardiac output in which the concentration of an intravascular tracer injected upstream is monitored by sampling downstream. This measurement is based on Equations 1 and 2. If the bolus could be injected in such a way that the outflow time-concentration curve was the shape of a rectangle, then the concentration (C) axis of this rectangle would be equal to M/V (Equation 2) where V is the discrete volume of blood within which the tracer is diluted. In turn, V = Q.T (Equation 2) where T is the duration of the rectangle and q is cardiac output.

Substituting for V,

$$Q = \frac{M}{C.T}. \qquad \text{Eq. 14}$$

Note that C.T is the area of the rectangle. The general form of this, the Stewart-Hamilton or indicator dilution curve,

$$\text{flow} = \frac{\text{mass injected or accumulated}}{\text{area under time-concentration curve}},$$

is used repeatedly in quantitative nuclear medicine in various settings.

For instance, consider measurement of blood clear-

ance of a tracer. Since blood clearance, Z, represents an equivalent flow of blood which is completely cleared of tracer, we can say

$$dM_t/dt = Z.C_a, \qquad \text{Eq. 15}$$

where M_t is the quantity of tracer removed from blood.

By integrating $$M_t = Z\int C_a(t).dt, \qquad \text{Eq. 16}$$

results in: $$Z = \frac{M_t}{\int C_a(t).dt}. \qquad \text{Eq. 17}$$

At infinite time, all the tracer will have left the blood so M_t will be equal to the injected dose and $\int C_a(t).dt$ the area to infinite time,

i.e., $$Z = \frac{\text{mass injected}}{\text{total area under clearance curve}}.$$

Note that Equation 17 does not specify instantaneous injection or the form of the plasma curve (i.e., monoexponential or multiexponential). Its most frequent clinical use is probably the measurement of the plasma clearance of renal agents such as ^{99m}Tc-DTPA for global GFR.

Instead of considering the quantity of tracer that has left the blood, we can look at the quantity M_b remaining in blood:

$$dM_b/dt = Q(C_v - C_a). \qquad \text{Eq. 18}$$

Z is that blood flow which would be completely cleared of tracer. So, if we say Q = Z, then $C_v = 0$,

i.e., $$dM_b/dt = -Z.C_a \qquad \text{Eq. 19}$$

(compare with Equation 15).

If the distribution volume, V, of the tracer is the intravascular space, such as a labeled colloid, then, from Equation 19,

$$\frac{dM_b}{dt} = -\frac{Z.M_b}{V} \qquad \text{Eq. 20}$$

According to Equation 20, dM_b/dt is proportional to M_b, so the blood concentration must decrease exponentially with rate constant Z/V and a tracer residence time in blood of V/Z.

An analogous approach can be adopted for the measurement of individual organ clearance from the rate of tracer uptake by the organ. Thus, from the Fick principle, we can say:

$$\frac{dM_t}{dt} = Q(C_a - C_v), \qquad \text{Eq. 21}$$

where M_t is the quantity of tracer taken up into the organ, Q is organ blood flow and C_a and C_v the tracer concentrations in arterial blood and the venous blood draining the organ, respectively. Note that the right hand side of Equation 21 is now positive, i.e., the organ tracer content is *increasing*.

If both sides of Equation 21 are multiplied by C_a, then extraction fraction, E, can be introduced into it.

Thus

$$\frac{dM_t}{dt} = \frac{Q(C_a - C_v).C_a}{C_a}, \qquad \text{Eq. 22}$$

but

$$E = \frac{C_a - C_v}{C_a}. \qquad \text{Eq. 23}$$

Therefore

$$\frac{dM_t}{dt} = (Q.E).C_a, \qquad \text{Eq. 24}$$

$$= Z.C_a. \qquad \text{Eq. 25}$$

Then Equation 25 can be integrated:

$$M_t = Z\int C_a(t).dt, \qquad \text{Eq. 26}$$

or

$$Z = \frac{M_t}{\int C_a(t)dt}$$

$$= \frac{\text{mass accumulated}}{\text{area under blood concentration time curve}}. \qquad \text{Eq. 27}$$

Equation 27 requires that the tracer accumulated in the organ remains within it. This may be true only for a limited period of time, such as DTPA in the kidney (about 3 min postinjection), but Z is still obtainable from Equation 27 up to this time (i.e., the mass accumulated at time t divided by the area under the blood disappearance curve up to time t) (Fig. 6). Note that the validity of Equation 27 is not affected by simultaneous uptake of tracer elsewhere.

Many quantitative techniques in nuclear medicine measure clearance of a tracer into a specific organ using this approach, especially in PET. The amount of tracer accumulated up to time t, M_t, can be measured by quantitative scanning or PET. Examples in PET are the measurement of myocardial blood flow with ^{13}N-labeled ammonia and ^{82}Rb (*8*) and the measurement of hepatic arterial blood flow with ^{13}N-labeled ammonia (*9*). The measurement of individual kidney GFR with ^{99m}Tc-DTPA is an example

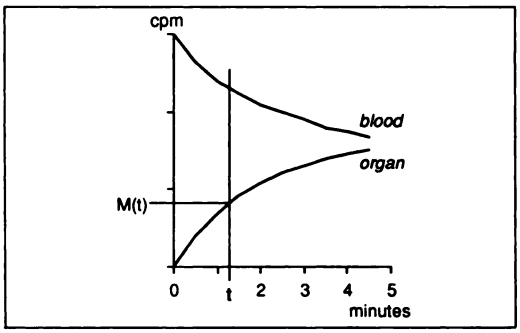

FIGURE 6. Idealized blood and organ time-activity curves, illustrating Equation 27. Thus, the organ clearance (ml/min) is the ratio of mass (MBq) accumulated up to time (t) and the area under the blood curve to the same time (min·MBq/ml), assuming no losses of tracer from the organ after uptake. If the organ takes up all injected activity, then clearance is also equal to the ratio of injected dose and the total area under the blood curve (compare with legends to Figs. 4 and 5).

in single photon work. Here, M_t, the renal activity, is measured up to about 3 min (after which the tracer leaves the kidney) and compared with the area under the plasma concentration-time curve up to time t (*10*). Alternatively, the differential equation (Equation 25), $dM_t/dt = Z.C_a$, may be used (*11*), but the principle is the same (Fig. 7).

Equation 26 can be further developed to arrive at the Patlak equation or Patlak plot (*12,13*). Thus, if Equation 26 is divided by C_a, then

$$\frac{M_t}{C_a} = \frac{Z\int C_a(t).dt}{C_a}. \qquad \text{Eq. 28}$$

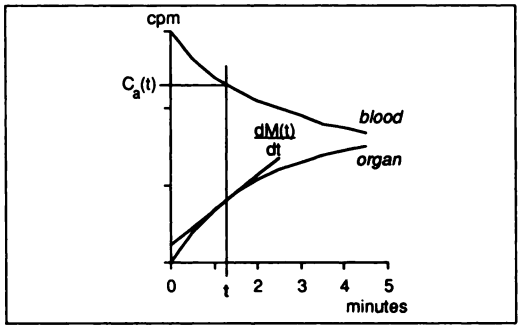

FIGURE 7. Same curves as in Figure 6 to illustrate Equation 25 which essentially states the Fick Principle.

Thus, $$\frac{dM}{dt} = Q(C_a - C_v)$$

but $$Q = Z/E \text{ and } E = (C_a - C_v)/C_a$$

so $$\frac{dM}{dt} = Z.C_a.$$

Integration of this equation gives Equation 27, which is illustrated in Figure 6.

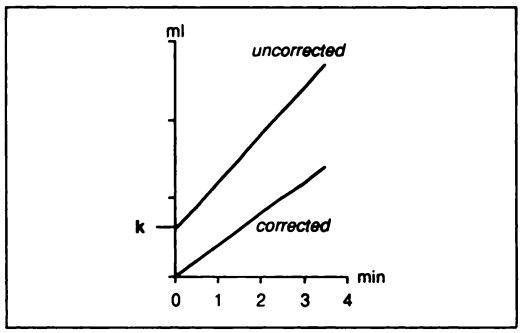

FIGURE 8. The Patlak plot (Equations 28 and 29) is applied to a ROI containing both an intravascular and extravascular background signal arising from a diffusible solute (e.g., ^{99m}Tc-DTPA). When regression is performed before any background subtraction, an intercept (k) is derived proportional to the intravascular background. The gradient of the regression includes a component reflecting the clearance of tracer into the extravascular space of background. After perfect background subtraction, the intercept is zero and the gradient proportional to clearance into the organ. Note that the unit of the y-axis is volume (see the units of the left hand side of Equation 28, whence MBq cancels out) and that of the x-axis, time. The latter is evident since this axis is the ratio of an area [$\int C_a(t).dt$] and the y-axis dimension [C_a] of that area. The y-axis of the Patlak plot is sometimes called normalized counts and the x-axis normalized time, particularly in the PET literature.

If the accumulated tracer remains within the organ, a graphical plot of M_t/C_a against $\int C_a(t).dt/C_a$ results in a straight line with slope Z (Fig. 8). The Patlak plot is frequently used in PET (e.g., measuring cerebral glucose utilization), but has also been used more recently in single photon work such as in the measurement of single kidney GFR, (*14,15*) hepatic and splenic colloid uptake (*16*), thyroidal iodine uptake (*17*) and regional permeability-surface area product (*18*).

The Patlak plot is attractive because of the convenient way in which it deals with blood background. Thus, if this blood background is a fraction, (k), of C_a, then the introduction of blood background into Equation 28 gives

$$\frac{M_t + k.C_a}{C_a} = \frac{Z\int C_a(t).dt + k.C_a}{C_a}$$

or

$$\frac{M_t + k.C_a}{C_a} = \frac{Z\int C_a(t).dt}{C_a} + k. \qquad \text{Eq. 29}$$

In other words, k is the zero time intercept of the Patlak plot performed without background subtraction but the slope remains equal to Z. In practice, for example in ^{99m}Tc DTPA renography, background also includes extravascular interstitial fluid into which DTPA diffuses simultaneously with glomerular filtration. The GFR

equivalent of this extravascular component of background is represented by the difference in the slope of the Patlak plot before and after background subtraction (Fig. 8).

MASS

In nuclear medicine, mass refers to those molecules that are radioactive and measured in molar becquerels. Occasionally it is left as an expression in its own right, as in the measurement of whole body exchangeable sodium. It is frequently combined with time or volume measurement as shown above in Equations 18–27.

QUANTIFICATION BY DIMENSIONLESS RATIOS

Many useful measurements in nuclear medicine are expressed in the form of a dimensionless ratio. Although the final ratio is unitless, most are arrived at by measurement of time, volume or mass, which cancel out in the ratio. An example of a dimensionless ratio which starts with measurement of mass is the fraction of cardiac output serving an organ. After injection into the left ventricle of radiolabeled microspheres, the activity accumulating in the kidney is measured by quantitative scanning. Expressed as a fraction of the injected dose, it is the fraction of cardiac output supplying the kidney. This measurement can be made noninvasively using a recirculating tracer (*19*). An example of one based on volume and time is the filtration fraction measured from the simultaneous clearances of ^{99m}Tc-DTPA and hippurate. These ratios have several advantages. They often have more physiological relevance than either component alone, such as renal blood flow-to-cardiac output. Second, they are often easier to measure because of the cancellation of terms common to both numerator and denominator.

A general technique from which several useful dimensionless ratios can be derived is whole body counting, either by the traditional method or by using an uncollimated gamma camera. The solid angle enclosing the face of the camera and a point source in the body at a distance of 4 m is relatively independent of the position of the source in a vertical axis. Because of the effect of photon attenuation, the count rate is dependent on the position of a point source in the axis perpendicular to the camera face. For whole body count measurements, the geometric mean has to be taken of the counts recorded with the patient respectively facing and turned from the camera. Depending on the radionuclide and the variable being measured, the patient is counted soon after administration of the tracer (when no losses can be assumed) and again at a later time. By either counting a standard at the same time as the patient or making a correction for physical decay of the radionuclide, the radioactivity lost from the body can be quantified as a fraction of the administered dose. Examples include the measurement of ^{111}In-labeled granulocyte excretion in inflammatory bowel disease (*20*) or bronchiectasis (*21*), the assessment of the entero-hepatic circulation using ^{75}Se-labeled SeHCAT (*22*) and the quantification of amyloid deposits in amyloidosis using ^{131}I-labeled serum amyloid P component (*23*).

CONCLUSION

Quantification in nuclear medicine is perceived, particularly by students, as a complex area only comprehensible to mathematics experts. As this review has shown, the subject largely can be encompassed by a few important relationships. Although this may jar with the purist, it is nevertheless clear that with a reasonable understanding, important and apparently complex concepts can be grasped, at least intuitively. Two simple rules will often help the novice to make sense of complicated equations. The first is to examine the units of the terms in the equations and to check that all units appear on both sides of the equation and cancel out. The second is to start with simple equations and increase their complexity as necessary rather than (this is particularly true of PET modelers) starting with complex equations and then simplifying them. Otherwise, the novice will not notice they have been simplified, for he or she will have given up by then.

REFERENCES

1. Zierler K. Equations for measuring blood flow by external monitoring of radioisotopes. *Circ Res* 1965;16:309–321.
2. Peters AM, Walport MJ, Bell RN, Lavender JP. Methods of measuring splenic blood flow and platelet transit time with ^{111}In-labeled platelets. *J Nucl Med* 1984;25:86–90.
3. Swinburne AJ, MacArthur CGC, Rhodes CG, Heather JD, Hughes JMB. Measurement of lung water in dog lobes using inhaled $C^{15}O_2$ and $H_2^{15}O$. *J Appl Physiol* 1982;52:1535–1544.
4. Thorburn GD, Kopald HH, Herd A, Hollenburg M, O'Morchoe CC, Barger AC. Intra-renal distribution of nutrient blood flow detected with Krypton-85 in the unanesthetised dog. *Circ Res* 1963;13:290–307.
5. Fazio F, Jones T. Assessment of regional ventilation by continuous inhalation of radioactive Krypton-81m. *Br Med J* 1975;3:673–676.
6. Paaske W. Microvascular exchange. Kinetic analysis of plasma disappearance curves. *Acta Chir Scand* 1980;Suppl 502:46–50.
7. Peters AM. Expressing glomerular filtration rate in terms of extracellular fluid volume. *Nephrol Dial Transplant* 1992;7:205–210.
8. Schelbert HR. Principles of positron emission tomography. In: Marcus ML, Schelbert HR, Skorton DJ, Wolf GL, eds. *Cardiac imaging*. Philadelphia: WB Saunders, 1991:1140–1168.
9. Chen BC, Huang S-C, Germano G, et al. Noninvasive quantification of hepatic arterial blood flow with nitrogen-13-ammonia and dynamic positron emission tomography. *J Nucl Med* 1991;32:2219–2228.
10. Britton KE, Brown NJG. *Clinical renography*; London: Lloyd-Luke. 1971.
11. Piepsz A, Dobbeleir A, Erbsmann F. Measurement of separate kidney clearance by means of ^{99m}Tc-DTPA complex and a scintillation camera. *Eur J Nucl Med* 1977;2:173–177.
12. Patlak CS, Blasberg RG, Fenstermacher JD. Graphical evaluation of blood to brain transfer constants from multiple time uptake data. *J Cereb Blood Flow Metab* 1983;3:1–7.
13. Hawkins RA, Phelps ME, Huang SC, et al. A kinetic evaluation of blood-brain barrier permeability in human brain tumors with gallium-68 EDTA and positron emission tomography. *J Cerebr Blood Flow Metab* 1984;4:507–515.
14. Rehling M, Moller ML, Lund JO, Jensen KD, Thamdrup B, Trap-Jensen J. Technetium-99m DTPA gamma camera renography: normal values and rapid determination of single kidney glomerular filtration rate. *Eur J Nucl Med* 1985;11:1–6.
15. Rutland MD. A comprehensive analysis of DTPA renal studies. *Nucl Med Commun* 1985;6:11–30.

16. Rutland MD. An analysis of the uptake of ^{99m}Tc sulphur colloid by liver and spleen. *Nucl Med Commun* 1984;5:593–602.
17. Decostre PL, Salmon Y. Temporal behavior of peripheral organ distribution volume in mammillary systems. A new tool for tracer analysis. *J Nucl Med* 1990;31:1702–1709.
18. Peters AM. Measurement of microvascular permeability to small solutes in man. Limitations of the technique. *Cardiovasc Res* 1990;24:504–509.
19. Peters AM, Brown J, Crossman D, et al. Noninvasive measurement of renal blood flow with ^{99m}Tc DTPA in the evaluation of patients with suspected renovascular hypertension. *J Nucl Med* 1990;31:1980–1985.
20. Carpani de Kaski M, Peters AM, Knight D, Stuttle AWJ, Lavender JP, Hodgson HJ. Indium-111 whole body retention: a new method for quantification of disease activity in inflammatory bowel disease. *J Nucl Med* 1992;33:756–762.
21. Currie DC, Saverymuttu SH, Peters AM, et al. Indium-111-labeled granulocyte accumulation in the respiratory tract of patients with bronchiectasis. *Lancet* 1987;1:1335–1339.
22. Merrick MV, Eastwood MA, Anderson JR, Ross HM. Enterohepatic circulation in man of a gamma-emitting bile acid conjugate 23-selena-25-homotaurocholic acid (SeHCAT). *J Nucl Med* 1982;23:126–130.
23. Hawkins PN, Wootton R, Pepys MB. Metabolic studies of radioiodinated serum amyloid P component in normal subjects and patients with systemic amyloidosis. *J Clin Invest* 1990;86:1862–1869.

(continued from page 694)

SELF-STUDY TEST
Gastrointestinal Nuclear Medicine

ANSWERS *(continued)*

2. Schwartz MJ, Lewis JH. Meckel's diverticulum: pitfalls in scintigraphic detection in the adult. *Am J Gastroenterol* 1984;78:611-618.

Items 8-11: Bleeding from a Rest of Ectopic Gastric Mucosa
Answers: 8, F; 9, F; 10, F; 11, F
This patient's images (Fig. 1) demonstrate active upper gastrointestinal bleeding, which is first seen on the 10-minute view (upper right image). A film from an upper gastrointestinal barium study (Fig. 2) demonstrates a 2-cm mucosal abnormality (white arrow) in the third portion of the duodenum. This was removed at surgery and histologically confirmed to be a site of bleeding in a focus of ectopic gastric mucosa.

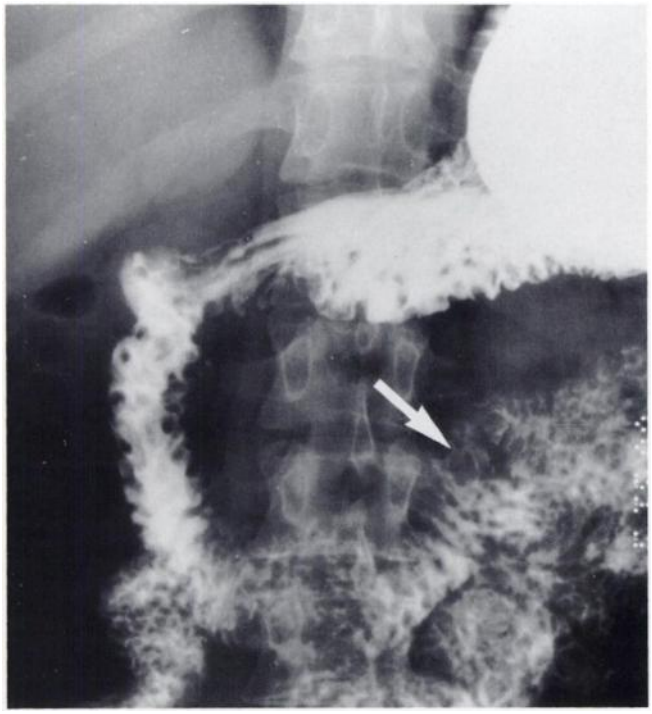

Figure 2. Upper gastrointestinal barium study of the patient whose ^{99m}Tc red blood cell scintigrams are shown in Test Figure 1. There is a filling defect in the barrium column in the third portion of the duodenum (arrow). This mass proved to be a rest of ectopic gastric mucosa.

This study was performed with red blood cells labeled by the "in vivtro" (modified in vivo) technique. The initial view at 5 minutes (upper left image) demonstrates tracer in the blood pool structures without significant gastric activity to suggest a large amount of free ^{99m}Tc pertechnetate or any area of active bleeding. By 10 minutes (upper right image), labeled red blood cells are now seen to have accumulated in the second and third portions of the duodenum. Over the next 20 minutes, extravasated activity moves quickly through the small bowel. Again, there is little gastric mucosal activity to suggest that small bowel activity is derived from free ^{99m}Tc pertechnetate. While the "in vivtro" method of red blood cell labeling is easy to perform and generally results in better labeling efficiency than the in vivo technique, 100% red blood cell labeling does not occur. When heparin is used as the anticoagulant during red blood cell labeling, ^{99m}Tc heparin complexes can accumulate in the kidney and urinary bladder (as in this patient). The bladder activity is not primarily due to free ^{99m}Tc pertechnetate. Excessive urinary activity is usually not a problem when the in vitro labeling method is used.

While gastrointestinal bleeding scintigraphy primarily has been used to identify sites of lower intestinal bleeding, sources of upper tract bleeding can be identified, as was true in this patient. This is one of the theoretical advantages of scintigraphy with labeled red blood cells versus that with ^{99m}Tc sulfur colloid; the latter has limited use in detecting upper gastrointestinal bleeding because hepatic and splenic activity often obscure sites of active bleeding in the upper abdomen.

Use of intravenous glucagon as an antispasmodic has been advocated by some to enhance visualization of bleeding sites in the small bowel. By decreasing small bowel motility, glucagon decreases the translocation of blood within the small bowel and, thus, the actively bleeding focus is more readily identifiable. The enhanced detection of bleeding sites may also be related to a vasodilatory effect of glucagon.

Occasionally, barium examination of the small bowel may be useful in identifying sites of gastrointestinal bleeding. The small bowel enteroclysis study is a specialized barium examination in which a gastric tube is fluoroscopically placed into the third or fourth portion of the duodenum and barium is instilled, followed by a mixture of saline and methyl cellulose. By precisely controlling the column of barium, optimal small bowel distention can be achieved and small bowel lesions, such as tumors, polyps, or Meckel's diverticula can be identified more readily.

References

1. Froelich JW, Juni J. Glucagon in the scintigraphic diagnosis of small bowel hemorrhage by Tc-99m-labeled red cells. *Radiology* 1984;151:239-243.
2. Maglinte DDT, Elmore MF, Isenberg M, Dolan PA. Meckel diverticulum: radiologic demonstration by enteroclysis. *AJR* 1980;134:925-933.

(continued on page 716)